Supplementary Information

Analytical model

Here, we present an analytical model based on that presented by Agrawal [1]. We consider an infinite population of haploid hermaphrodites with discrete non-overlapping generations. Individuals are characterized by the same two loci as in the simulation model. Because we are interested in maternal infection, we must keep track of an individual's ancestry at the **A**-locus. Therefore, we let $x_{i,j;k}$ denote the frequency of genotype (i, j) individuals that are born to a mother with antigen genotype k. The pair of indices (i, j) denotes the individual's genotypes at the **A**-locus and **M**-locus, respectively. For example, $x_{A,M;a}$ denotes the frequency of individuals of genotype (A, M) born to mothers of genotype a.

Each generation individuals first reproduce sexually. During reproduction, mutation occurs between alternative alleles at the antigen locus with probability μ_j, where j denotes an individual's genotype at the modifier locus ($j = m$ or $j = M$). The frequency of eggs of genotype (i, j) produced by mothers of antigen type k is, therefore, given by

$$e_{i,j;k} = \sum_g \left((1 - \mu_j)\delta_{i,k} + \mu_j(1 - \delta_{i,k}) \right) x_{k,j;g} \,, \tag{S1}$$

where $\delta_{i,k}$ is an indicator function that equals 1 if $i = k$ and 0 if $i \neq k$. The sum over g sums over all possible grandmother types (i.e. all ancestry classes for mothers of genotype (k, j)). Similarly, the frequency of sperm of genotype (i, j) is given by

$$s_{i,j} = \sum_{k,g} \left((1 - \mu_j)\delta_{i,k} + \mu_j(1 - \delta_{i,k}) \right) x_{k,j;g} \,. \tag{S2}$$

Note that we assume there is no paternal transmission, and so we do not track the ancestry of the father. Summing over all sperm donors' antigen types (i.e. over all k), in addition to over all grandmother types, accomplishes this.

Sperm and eggs are assumed to unite randomly and in proportion to their frequencies. We let $f_{(m,n;o)\times(p,q)} = e_{m,n;o}s_{p,q}$ denote the frequency of unions between $(m,n;o)$ eggs and (p,q) sperm. These unions produce transient diploids that then undergo meiosis, with recombination occurring between loci at rate r. The genotype frequencies after meiosis are given by

$$x'_{i,j;k} = \sum_{m,n,o,p,q} f_{(m,n;o)\times(p,q)} \Psi_{i,j;k,(m,n;o)\times(p,q)} \,, \tag{S3}$$

where $\Psi_{i,j;k,(m,n;o)\times(p,q)}$ is the fraction of offspring of type $(i,j;k)$ resulting from meiosis with recombination of the transient diploid produced by the union of $(m,n;o)$ eggs and (p,q) sperm.

Selection follows reproduction. There are two primary components to selection in our model. First, we assume there is maternal infection, in the form of similarity selection, as described above. An individual that differs from its mother at the **A**-locus will have similarity fitness (denoted w_S) equal to 1, while an individual with the same genotype will have similarity fitness $w_S = 1 - \gamma$. By imposing a penalty for sharing the same allele as one's mother at the **A**-locus, we are implicitly adopting an immunity model in which parasites target hosts on the basis of genotype, such as the matching alleles model used in the simulations.

Second, we assume that there is "genotypic selection" at the **A**-locus. This component of an individual's fitness represents selection imposed by the global parasite pool and is, therefore, independent of ancestry. We assign genotypic fitnesses (w_G) of 1 and $1 - \alpha$ to the A and a alleles, respectively. When α is positive (respectively, negative), individuals with an A allele have a higher (respectively, lower) genotypic fitness. For convenience,

we assume that α is positive in what follows. Although fluctuations in genotypic selection would be expected in a model of host-parasite coevolution under many parameter regimes, as observed in our simulations (Fig. 2) and in previous work [2], for sake of tractability, we do not allow such fluctuations to occur here. Our analytical model, therefore, approximates the dynamics that would occur during periods when parasites that can infect individuals with the a-allele predominate.

The above two fitness components act multiplicatively to determine an individual's total fitness. An individual with genotype i at the **A**-locus, born to a mother with allele k at the **A**-locus, has fitness

$$w_{i;k} = w_S w_G = (1-\gamma)^{\delta_{i,k}}(1-\alpha)^{\delta_i}\,, \tag{S4}$$

where $\delta_{i,k}$ equals 0 when $i \neq k$ and 1 when $i = k$, and δ_i equals 0 when $i = A$ and 1 when $i = a$. The genotype frequencies after selection can then be computed as

$$x''_{i,j;k} = \frac{x'_{i,j;k} w_{i;k}}{\bar{w}}\,, \tag{S5}$$

where $\bar{w}$ is the mean fitness $\bar{w} = \sum_{i,j,k} x'_{i,j;k} w_{i;k}$.

As described in the main text, a basic extension to parasites entails a change to the fitness functions, such that having the same genotype as one's mother is advantageous. Specifically this means replacing the fitness function of Eq. S4 with

$$w_{i;k} = w_S w_G = (1-\gamma)^{1-\delta_{i,k}}(1-\alpha)^{\delta_i}\,, \tag{S6}$$

QLE analysis

We performed a QLE (Quasi-Linkage Equilibrium) analysis to examine the rate at which evolution occurs at the modifier locus [3]. Briefly, the QLE analysis assumes that selection and mutation are weak relative to recombination and segregation and thus that allele frequency changes at the **A** and **M** loci occur slower than changes in the various associations among the loci (e.g., linkage disequilibrium). Using this separation of time scales allows us to assume that the associations are always at their steady-state values, which greatly simplifies analysis.

We assume that the modifier allele, M, has an effect of increasing the mutation rate by $\Delta\mu$ from the baseline value μ_m encoded by the m allele (i.e., $\mu_M = \mu_m + \Delta\mu$). In order to perform the QLE analysis, we assume that selection and mutation are weak relative to recombination. We begin by following Agrawal (2006) and assuming that α is on the order of some small term, ζ, and that γ is of even smaller order, ζ^2. We further assume that the mutation rate, μ_m, and the effect of the modifier, $\Delta\mu$, are also of order ζ^2. Due to these assumptions, changes in allele frequency occur much more slowly than changes in association measures such as linkage disequilibrium (shown below). Thus it is a reasonable approximation to assume that the latter quickly converge to their steady-state values.

To leading order, ζ, we find that the change in frequency of the A-allele over a single generation is equal to

$$\Delta P_A = \alpha V_A \zeta + O(\zeta^2)\,, \tag{S7}$$

where V_A is the variance at the **A**-locus, which is analogous to Eq. 2 in Agrawal (2006). The change in frequency of the M-allele is

$$\Delta P_M = D_{A,M}\alpha(1-r)\zeta + O(\zeta^2) \tag{S8}$$

where $D_{A,M}$ is the linkage disequilibrium between the **A** and **M** loci in the offspring. We next find the steady-state value of $D_{A,M}$ to substitute into Eq. S8. To do this, we solve the system of equations that results from setting the change in each association measure over a single generation equal to zero. Because these equations are too complex to solve exactly, we first approximate the change that occurs over a single time-step with a Taylor series expansion. The recursions, to leading order are

$$\begin{aligned}
\Delta D_{A,M} &= -rD_{A,M} + O(\zeta) \\
\Delta D_{A;A} &= -D_{A;A} + \frac{V_A}{2} + O(\zeta) \\
\Delta D_{M;A} &= -D_{M;A} + \frac{1}{2}D_{A,M} + O(\zeta) \\
\Delta D_{A,M;A} &= -D_{A,M;A} + \frac{1}{2}(1-r)(1-2P_A^{\mathrm{Mom}})D_{A,M} + O(\zeta)\,.
\end{aligned} \tag{S9}$$

where the letters before the semicolon in the subscripts refer, respectively, to the antigen and modifier alleles in the offspring and the letter after the semicolon refers to the antigen allele of the mother. For example, $D_{A,M}$ is the linkage disequilibrium in offspring individuals, and $D_{A;A}$ is the association between antigen genotypes in offspring and their mothers. All the changes are of order 1, which, compared to the order of allele frequency changes at the **A** and **M** loci given below, demonstrates that these associations reach steady-state rapidly, as assumed in a QLE analysis. Only $D_{A,M}$ turns out to matter in our analysis, because it is the only association which appears in Eq. S8. To the order of precision presented in Eq. S9, $D_{A,M}$'s steady-state solution is equal to zero, so we must look at higher order terms. Including terms up to order ζ^2, and again setting the recursions equal to zero yields the steady-state solution

$$D_{A,M} = \frac{2(1-r)}{r}\Delta\mu(1/2 - P_A)V_M\zeta^2 + O(\zeta^3), \tag{S10}$$

where V_M is the variance at the **M**-locus. Similarly computing ΔP_M to higher order and substituting this steady-state value for $D_{A,M}$ yields

$$\Delta P_M = \frac{2(1-r)}{r}\alpha\Delta\mu(1/2 - P_A)V_M\zeta^3 + O(\zeta^4)\,. \tag{S11}$$

From Eq. S11, we can see that the rate and direction of change in the modifier depends only on the strength of genotypic selection (α), and that higher mutation rates are selected against when the beneficial A-allele is at a frequency greater than $1/2$. We can also see that lower rates of recombination, r, and a larger effect size of the modifier, $\Delta\mu$, always increase the strength of selection on the modifier. In contrast to Agrawal's findings for modifiers of sex, the strength of similarity selection, γ, does not appear in these equations. Even with α of higher order than γ, he found them to have comparably strong effects on the evolution of sex (see his Eq. 3). This led him to conclude that similarity selection is a more potent force than genotypic selection for the evolution of sex. As he explained, this is because similarity selection acts on higher order genetic associations (those between mothers and offspring) than genotypic selection (those between copies of alleles in diploid individuals). In our case, however, mutation affects mother-offspring associations at the antigen locus (what similarity selection acts on) to the same order as it directly modifies antigen alleles that characterize individuals (what genotypic selection acts on). Hence the order of magnitudes of the effects of similarity and genotypic selection on mutation rate evolution are the same, as we confirm below.

Because we are interested in the combined effects of genotypic selection, α, and similarity selection, γ, on the evolution of mutation rate, we proceed by conducting another QLE analysis in which α and γ are of the same order. In particular α and γ are on the order of some small term, ζ, and the rest of the analysis is conducted as described above.

To leading order, ζ, we now find that the change in frequency of the A-allele over a

single generation is equal to

$$\Delta P_A = V_A(\alpha + \gamma(1/2 - P_A))\zeta + O(\zeta^2) \tag{S12}$$

and the change in frequency of the M-allele is

$$\Delta P_M = D_{A,M}\left((1-r)\alpha + \gamma(1/2 - P_A)\right)\zeta + O(\zeta^2) \tag{S13}$$

Repeating what we did in the first QLE analysis, we find that the recursions for the association measures over one time step are the same as those in Eq. S9 and that the steady-state solution for $D_{A,M}$ is the same as in Eq. (S10). Repeating the procedure described above, we find the leading order change in the frequency of the M-allele to be

$$\Delta P_M = 2\Delta\mu V_M \left(\frac{1-r}{r}\right)\left(\alpha\left(1/2 - P_A\right) + \gamma((1/2 - V_A)(r + 1/2) - V_A/2)\right)\zeta^3 + O(\zeta^4) \tag{S14}$$

From Eq. (S14) we can see that the rate and direction of change in the modifier depends on both the strength of similarity selection, γ, and the strength of genotypic selection, α. We can also see that lower rates of recombination, r, and a larger effect size of the modifier, $\Delta\mu$, always increase the strength of selection on the modifier. However, the effect of r on reducing the rate of increase of a modifier is dampened when similarity selection, γ, is stronger. For more discussion of these results see Section 5 in the main text.

References

[1] Agrawal, A. F. 2006 Similarity selection and the evolution of sex: revisiting the Red Queen. *PLoS Biol.*, **4**, 1364–1371.

[2] Nee, S. 1989 Antagonistic co-evolution and the evolution of genotypic randomization.

J. Theor. Biol., **140**, 499–518.

[3] Barton, N. H. & Turelli, M. 1991 Natural and sexual selection on many loci. *Genetics*, **127**, 229–255.

Variables and Parameters	Definitions
$e_{i,j;k}$	Frequency of eggs of genotype (i,j) produced by mothers of antigen type k.
$f_{(m,n;o)\times(p,q)}$	The frequency of unions between $(m,n;o)$ eggs and (p,q) sperm.
r	Recombination rate between the **A**-locus and **M**-locus.
$s_{i,j}$	Frequency of sperm of genotype (i,j).
v	Fitness cost in hosts of being infected in the simulation model.
$w_{i;k}$	Total fitness of an individual.
$x_{i,j;k}$	Frequency of genotype (i,j) individuals that are born to a mother with antigen type k.
α	Genotypic fitness penalty of having allele a.
γ	Similarity fitness penalty for an individual that is the same as its mother at the **A**-locus.
θ	The probability that an encounter with a compatible parasite causes an infection in the global infection stage.
μ_i^S	Mutation rate of individuals of species S with allele i at the **M**-locus.
ϕ	The probability that an encounter with a compatible parasite causes an infection in the maternal infection stage.
$\Delta\mu$	Effect size of the mutation rate modifier allele.
$\Psi_{i,j;k,(m,n;o)\times(p,q)}$	The fraction of offspring of type $(i,j;k)$ resulting from meiosis of the transient diploid produced by the union of $(m,n;o)$ eggs and (p,q) sperm.

Table S1: Model Parameters and Variables.

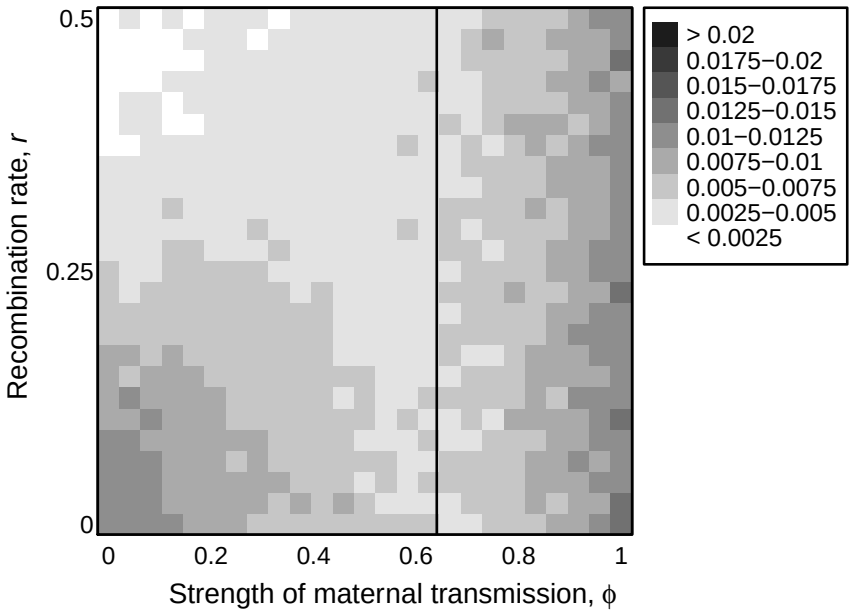

Figure S1: Evolved mutation rate in hosts after 10^7 generations as a function of the recombination rate. Each cell again represents the mean of 10 replicate simulations. To the right of the vertical black line, cycle amplitude in hosts is negligible for the duration of the evolution runs . In Fig. S2, we show vertical cross sections from this figure for $\phi = 0.1$ and $\phi = 0.9$ with hundred-fold replication. $v = 0.25$ and all else is as described in Fig. 3.

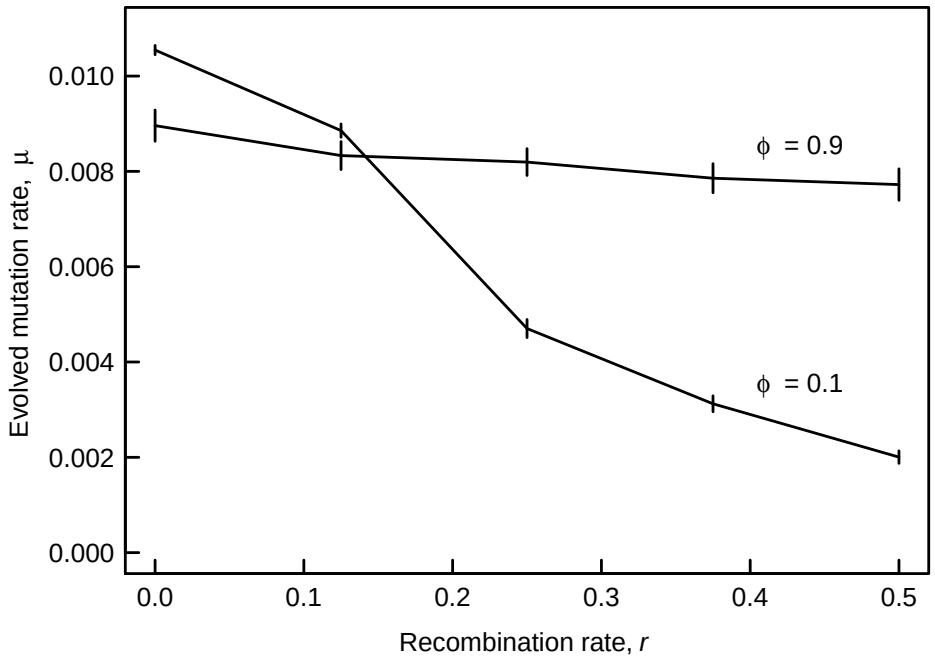

Figure S2: Evolved mutation rate as a function of recombination rate, r, for two rates of maternal transmission, ϕ. The value of each point is the mean mutation rate that evolved after 10^7 generations over 100 replicate runs. It can be seen here that high recombination weakens selection on modifiers that increase mutation rate for both weak and strong maternal transmission, but that this reduction is much smaller in the latter case. This is not evident in Fig. S1 where there is less replication. Vertical bars denote standard errors. All other parameters are as in Fig. S1.

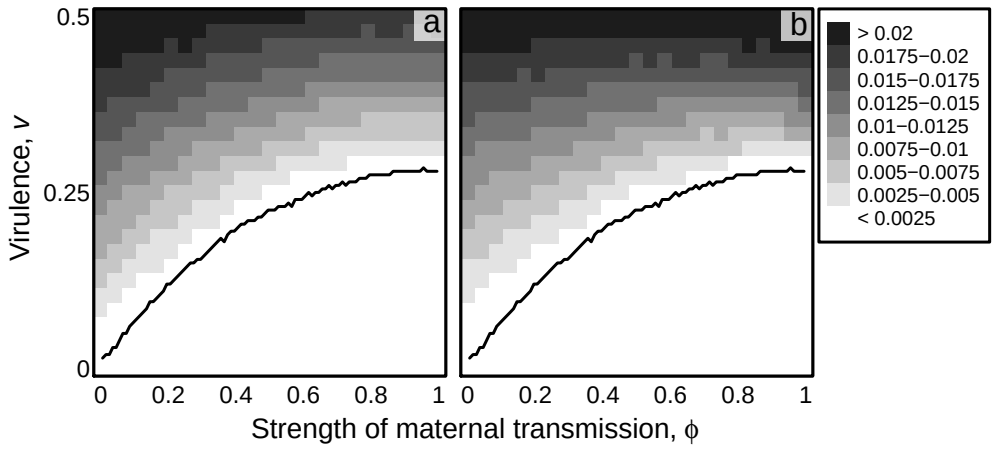

Figure S3: The critical mutation rate at which cycle size becomes negligible (amplitude$<$ 0.1) in hosts (**a**) and parasites (**b**). All other parameters are as in Fig. 1

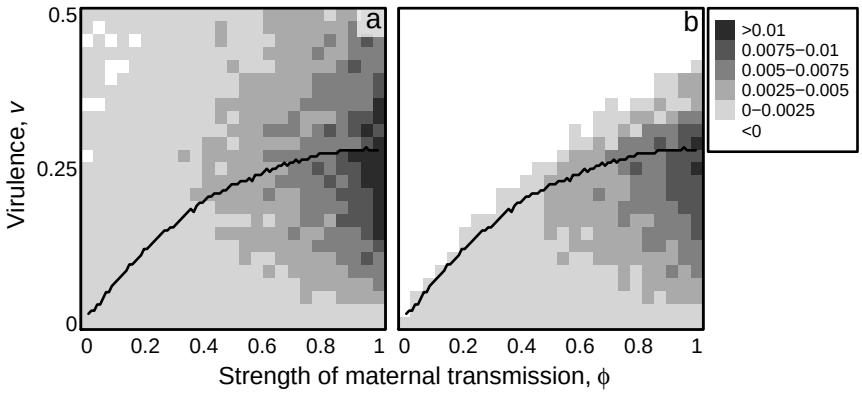

Figure S4: The difference, in hosts, between the mutation rates that evolved (i.e., those shown in Fig. 3) and the critical mutation rate at which coevolutionary cycles become negligible (amplitude < 0.1) with (**a**) complete linkage ($r = 0$) and (**b**) free recombination ($r = 0.5$). Darker shading indicates that mutation rates evolved further past the critical mutation rate and white cells indicate cases when evolved mutation rates failed to reach the critical value. The critical mutation rate at which cycle amplitude becomes negligible is shown in Fig. S3a. Previous theory has shown that mutation rates will evolve until cycles become negligible. Here we show that, with sufficiently strong maternal transmission, mutation rates will evolve past this critical value. The solid curves indicate the boundary below which cycle amplitude is negligible, even with small mutation rates (see Fig. 2.

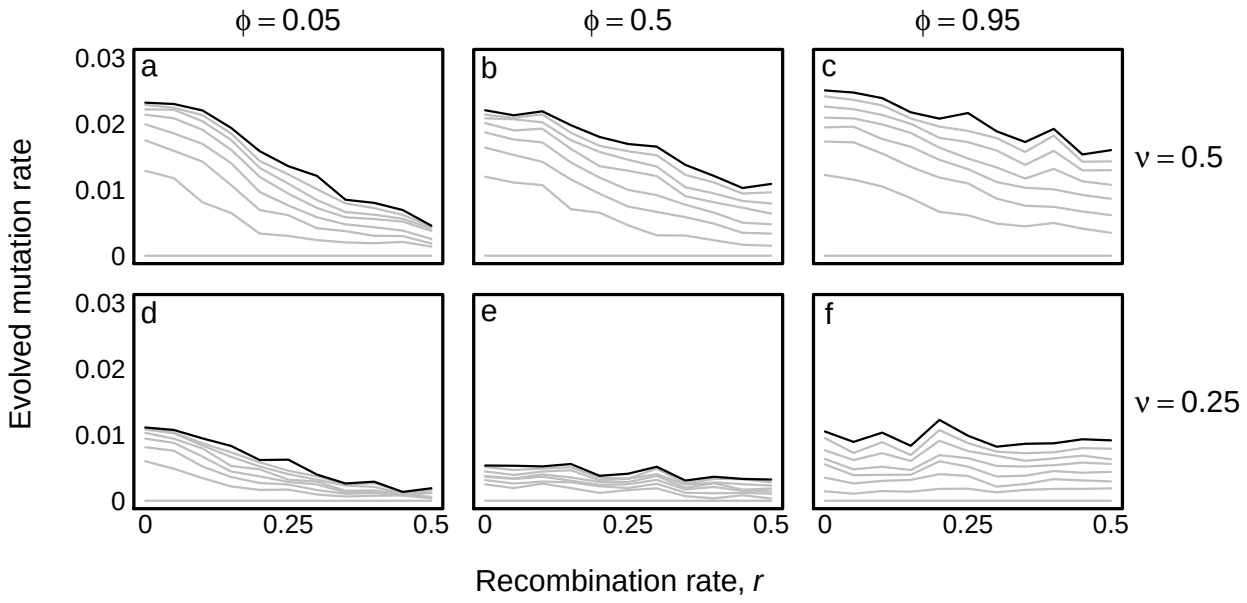

Figure S5: Time course for the evolution of mutation rate in hosts for varying rates of maternal infection, ϕ, and virulence, v. Parameters used for the six panels here correspond to the analogous six panels in Fig. 1. The black curve denotes the mutation rate that evolved after 10^7 generations, averaged across 10 replicate model runs, and the grey curves denote the evolved mutation rate at uniformly spaced intermediate time intervals. As can be seen here, modifier evolution has dramatically slowed by generation 10^7, except in the case when maternal transmission is strong (panels c and f).

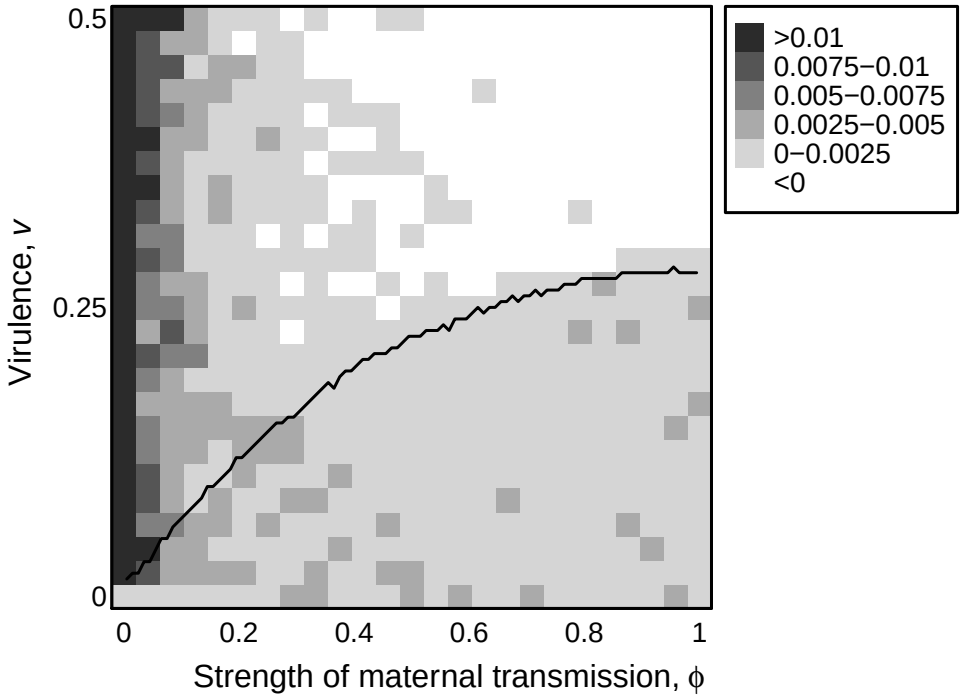

Figure S6: The difference, in parasites, between the ESS mutation rates (i.e., those shown in Fig. 5b) and the critical mutation rate at which coevolutionary cycles (measured for consistency from host dynamics) become negligible (amplitude < 0.1). Darker shading indicates that mutation rates evolved further past the critical mutation rate and white cells indicate cases when evolved mutation rates failed to reach the critical value. The critical mutation rate at which cycle amplitude becomes negligible is shown in Fig. S3b. Previous theory has shown that mutation rate in parasites will also evolve until cycles become negligible. Here we show that, with sufficiently strong maternal transmission, mutation rates in parasites will stop evolving before reaching this critical value. The solid curve indicates the boundary below which cycle amplitude in hosts is negligible, even with very small mutation rates in both species (see Fig. 2). In this region, any mutation rate evolution that occurs in parasites will, thus, lead to a positive value, even if it is occurring only by drift.